ASSUMED-STRAIN FINITE ELEMENT TECHNIQUE FOR ACCURATE MODELLING OF PLASTICITY PROBLEMS

E. ARTIOLI[*], G. CASTELLAZZI[†] AND P. KRYSL[♯]

* Department of Civil Engineering and Computer Science (DICII)
University of Rome "Tor Vergata"
Via del Politecnico 1, 00133 Roma, Italy
e-mail: artioli@ing.uniroma2.it, web page: http://www.dicii.uniroma2.com/

[†]Department of Civil, Chemical, Environmental and Material Engineering (DICAM)
University of Bologna
V.le Risorgimento 2, 40136 Bologna, Italy
e-mail: giovanni.castellazzi@unibo.it - Web page: http://www.unibo.it

[♯] Department of Structural Engineering
University of California, San Diego
9500 Giman Dr ♯0085, La Jolla, CA 92093-0085, U.S.A.
e-mail: pkrysl@ucsd.edu - Web page: http://structures.ucsd.edu

Key words: Assumed-strain gradient, NICE formulation, nodal integration, von-Mises plasticity, midpoint integration algorithm.

Abstract. In this work a linear hexahedral element based on an assumed-strain finite element technique is presented for the solution of plasticity problems. The element stems from the NICE formulation and its extensions. Assumed gradient operators are derived via nodal integration from the kinematic-weighted residual; the degrees of freedom are only the displacements at the nodes. The adopted constitutive model is the classical associative von-Mises plasticity model with isotropic and kinematic hardening; in particular a double-step midpoint integration algorithm is adopted for the integration and solution of the relevant nonlinear evolution equations. Efficiency of the proposed method is assessed through simple benchmark problem and comparison with reference solutions.

1 INTRODUCTION

An assumed-strain finite element technique for the solution of plasticity models is presented. The element stems from the NICE formulation [1] and its further extensions [2, 3] that uses the weighted residual method to enforce weakly the balance equation with the natural boundary condition and also the kinematic equation that links the element-wise and the assumed-deformation gradient. Assumed gradient operators are derived via

nodal integration from the kinematic-weighted residual. Since the assumed-deformation gradients are expressed entirely in terms of the nodal displacements, the degrees of freedom are only the primitive variables (displacements at the nodes). In this work the *NICE-H8* 8-node hexahedral element is investigated. The adopted constitutive model is classical von-Mises plasticity in the realm of small deformation. A double-step midpoint integration algorithm is also presented for the integration and solution of the relevant nonlinear evolution equation for the plastic strain tensor [4]. The performances of the proposed approach are illustrated by means of a classical benchmark.

2 Weighted residual formulation of small-displacement, snall-strain deformation

We consider the model of small-displacement, small-strain deformation governed by the following equations:

$$\mathbf{B}^T \boldsymbol{\sigma} = \widetilde{\mathbf{b}}, \tag{1}$$

$$\boldsymbol{\sigma} = \frac{\partial \mathcal{W}}{\partial \boldsymbol{\varepsilon}} \tag{2}$$

$$\boldsymbol{\varepsilon} = \mathbf{B}\mathbf{u}, \tag{3}$$

in Ω, together with the following boundary conditions

$$(\mathbf{u})_i = (\widetilde{\mathbf{u}})_i \quad \text{on } \partial\Omega_{u,i}, \tag{4}$$

$$(\mathbf{N}^{\mathrm{T}}\boldsymbol{\sigma})_i = (\widetilde{\mathbf{t}})_i \quad \text{on } \partial\Omega_{t,i} \quad \text{for } i = 1, 2, 3. \tag{5}$$

In the above equations, $\mathbf{u}$ is the displacement vector, $\boldsymbol{\varepsilon}$ and $\boldsymbol{\sigma}$ are the vectors of strain and stress respectively, $\mathbf{B}$ and $\mathbf{B}^T$ are linear differential operators of symmetric gradient and divergence respectively, $\mathbb{D}$ is a symmetric positive definite material stiffness matrix, $\widetilde{\mathbf{b}}$ is a prescribed body load term, $\mathbf{N}$ is the outward unit normal vector on $\partial\Omega$, and $\widetilde{\mathbf{u}}$ and $\widetilde{\mathbf{t}}$ are the prescribed displacements and prescribed tractions. Following the derivation presented by Castellazzi and Krysl [3], the model problem described above is recast in the form of a saddle-point problem given by the following equations:

$$\mathcal{R}_{Bt} = \delta\mathcal{R}(\mathbf{u}, \bar{\boldsymbol{\varepsilon}}) \cdot \delta\mathbf{u} = \int_\Omega \left[\delta\mathbf{u}^T \mathbf{B}^T \frac{\partial \mathcal{W}}{\partial \bar{\boldsymbol{\varepsilon}}} - \delta\mathbf{u}^{\mathrm{T}}\widetilde{\mathbf{b}} \right] dV - \int_{\partial\Omega_t} \delta\mathbf{u}^{\mathrm{T}}\widetilde{\mathbf{t}} dS = 0,$$

$$\mathcal{R}_K = \delta\mathcal{R}(\mathbf{u}, \bar{\boldsymbol{\varepsilon}}) \cdot \delta\bar{\boldsymbol{\varepsilon}} = \int_\Omega \delta\bar{\boldsymbol{\varepsilon}}^T \mathbb{D} \left(\mathbf{B}\mathbf{u} - \bar{\boldsymbol{\varepsilon}} \right) dV = 0.$$

where $\mathbb{D} = \partial^2 \mathcal{W}/\partial\bar{\boldsymbol{\varepsilon}}^2$ is the tangent stiffness of the material. The two conditions above represent the weighted residuals of the balance + traction boundary condition and the kinematic equation.

In the present context, the strains $\bar{\boldsymbol{\varepsilon}}$ and $\delta\bar{\boldsymbol{\varepsilon}}$ are derived from the displacement field using a special gradient operator and therefore are assumed in the form

$$\bar{\boldsymbol{\varepsilon}} = \overline{\mathbf{B}}\mathbf{u}, \quad \delta\bar{\boldsymbol{\varepsilon}} = \overline{\mathbf{B}}\delta\mathbf{u} \tag{6}$$

where $\overline{\mathbf{B}}$ is the assumed strain-displacement operator. Consequently, we can write the weak problem of finding $\mathbf{u}$, $\overline{\mathbf{B}}$ that satisfy the balance residual

$$\mathcal{R}_{Bt} = \delta\mathcal{R}(\mathbf{u}, \bar{\boldsymbol{\varepsilon}}) \cdot \delta\mathbf{u} = \int_\Omega \left[\delta\mathbf{u}^T \mathbf{B}^T \frac{\partial\mathcal{W}}{\partial(\overline{\mathbf{B}}\mathbf{u})} - \delta\mathbf{u}^{\mathrm{T}}\widetilde{\mathbf{b}} \right] dV - \int_{\partial\Omega_t} \delta\mathbf{u}^{\mathrm{T}}\widetilde{\mathbf{t}} dS = 0, \qquad (7)$$

and the kinematic residual

$$\mathcal{R}_K = \int_\Omega (\mathbf{B}\delta\mathbf{u})^{\mathrm{T}} \, \mathbb{D} \left(\mathbf{B}\mathbf{u} - \overline{\mathbf{B}}\mathbf{u} \right) dV = 0, \qquad (8)$$

where the test function $\delta\mathbf{u}$ is designed to vanish along the parts of the boundary $\partial\Omega_u$ (where essential boundary conditions are prescribed). Note that both conditions are now expressed in terms of the unknown displacement field, operated upon by both the symmetric gradient and the assumed symmetric gradient: the role of the assumed strain is now carried by the (at this point undetermined) assumed strain-displacement gradient operator $\overline{\mathbf{B}}$.

Introducing a finite element approximation for $\mathbf{u} = \sum_I N_I \mathbf{u}_I$, and $\eta = \sum_I N_I \boldsymbol{\eta}_I$, where N_I are suitable finite element basis functions, the discrete kinematic weighted residual equation (8) becomes

$$\sum_{I,J} \boldsymbol{\eta}_I^T \left(\int_\Omega \overline{\mathbf{B}}_I{}^T \mathbb{D} (\overline{\mathbf{B}}_J - \mathbf{B}_J) \, dV \right) \mathbf{u}_J = 0 . \qquad (9)$$

where we have introduced the strain-displacement matrices $\mathbf{B}_J = \mathbf{B}(N_J)$, defined element-by-element, and the, as yet unknown, strain-displacement matrices $\overline{\mathbf{B}}_I$ that are used to produce the assumed test and trial strains.

The kinematic residual was used by Krysl and Zhu [1] to design the assumed-strain gradient operator, $\overline{\mathbf{B}}$, from the condition that such operator should satisfy *a priori* the kinematic residual statement. The derivation proceeds directly by discretizing the residual with finite elements, in the present case with eight-node hexahedral finite elements, termed in the following NICE-H8, and thereby obtaining the *discrete* assumed-strain operators.

Nodal quadrature is performed at the nodes in the volume integrals. For the hexahedron used in the present work the nodal quadrature rule is easily specified as

$$\int_V (\bullet)(\mathbf{x}) \, dV \approx \sum_e \sum_{K \in \text{nodes}(e)} (\bullet)(\mathbf{x}_K) \mathcal{J}(\mathbf{x}_K) w_K , \qquad (10)$$

where e iterates all the elements in the mesh, K runs over all the quadrature points in the element. Furthermore $\mathbf{x}_K$ is the location of the quadrature point (node), $\mathcal{J}(\mathbf{x}_K)$ is the Jacobian of the isoparametric mapping, and w_K is the weight of the quadrature point. In this case, the quadrature points coincide with the nodes, and the weights are all equal to one (if we assume that the standard shape is a tensor product of three bi-unit intervals).

Omitting details for brevity's sake, the assumed-strain nodal matrix is finally obtained as a weighted average of the elementwise strain-displacement matrices

$$\overline{\mathbf{B}}_J = \frac{\sum_{e \in \text{elems}(K)} \mathcal{J}(\mathbf{x}_K) w_K \mathbf{B}_J(\mathbf{x}_K)}{\sum_{e \in \text{elems}(K)} \mathcal{J}(\mathbf{x}_K) w_K} . \tag{11}$$

It is noted that the stiffness matrix is symmetric, since

$$\int_V \overline{\mathbf{B}}_I{}^T \mathbb{D} \overline{\mathbf{B}}_J \, \mathrm{d}V = \int_V \overline{\mathbf{B}}_I{}^T \mathbb{D} \mathbf{B}_J \, \mathrm{d}V = \int_V \mathbf{B}_I{}^T \mathbb{D} \overline{\mathbf{B}}_J \, \mathrm{d}V . \tag{12}$$

3 Midpoint integration algorithm for von-Mises plasticity

3.1 Constitutive equations

We consider small strain von-Mises plasticity with linear isotropic and kinematic hardening [5, 6]. Splitting of stress and strain tensors, $\boldsymbol{\sigma}$ and $\boldsymbol{\varepsilon}$, into deviatoric and volumetric parts gives:

$$\boldsymbol{\sigma} = \mathbf{s} + p\mathbf{I} \qquad \text{with} \qquad p = \frac{1}{3}\mathrm{tr}\boldsymbol{\sigma} \tag{13}$$

$$\boldsymbol{\varepsilon} = \mathbf{e} + \frac{1}{3}\theta\mathbf{I} \qquad \text{with} \qquad \theta = \mathrm{tr}\boldsymbol{\varepsilon} \tag{14}$$

where tr indicates the trace operator, while $\mathbf{I}$, $\mathbf{s}$, p, $\mathbf{e}$, θ are respectively the second order identity tensor, the deviatoric and volumetric stress, the deviatoric and volumetric strain.

The constitutive equations governing material behavior are

$$
\begin{align}
p &= K\theta \tag{15}\\
\mathbf{s} &= 2G(\mathbf{e} - \mathbf{e}^p) \tag{16}\\
\boldsymbol{\Sigma} &= \mathbf{s} - \boldsymbol{\alpha} \tag{17}\\
F &= \|\boldsymbol{\Sigma}\| - \sigma_y \tag{18}\\
\dot{\mathbf{e}}^p &= \dot{\gamma}\mathbf{n} \tag{19}\\
\sigma_y &= \sigma_{y,0} + H_{iso}\gamma \tag{20}\\
\dot{\boldsymbol{\alpha}} &= H_{kin}\dot{\gamma}\mathbf{n} \tag{21}\\
\dot{\gamma} &\geq 0 , \quad F \leq 0 , \quad \dot{\gamma}F = 0 \tag{22}
\end{align}
$$

where K is the material bulk modulus, G is the material shear modulus, $\mathbf{e}^p$ is the traceless plastic strain, $\boldsymbol{\Sigma}$ is the relative stress in terms of the backstress $\boldsymbol{\alpha}$, introduced to describe the shifting of the yield surface in deviatoric stress space due to kinematic hardening. Moreover, F is the von-Mises yield function, $\mathbf{n}$ is the normal to the yield surface, σ_y is the yield surface radius, $\sigma_{y,0}$ the initial yield stress, H_{kin} and H_{iso} are the kinematic and isotropic linear hardening moduli. equations (22) are the so-called Kuhn-Tucker loading

conditions, which render the constitutive model under consideration a non-smooth convex optimization problem [7]. In particular, the second equation limits the relative stress within the admissible convex set bounded by the yield surface $F = 0$, while the other two determine the type of loading phase the material is experiencing, namely *elastic* when $F < 0\,\dot{\gamma} = 0$, and *plastic* when $F = 0\,\dot{\gamma} > 0$, respectively. It is noted that the constitutive equation relating the volumetric part of stress and strain is linear, thus the numerical schemes treated in the following deal only with the deviatoric part of the model.

In the following we resume a double-step midpoint integration algorithm for the integration and solution of the constitutive model within a strain-driven framework. The problem at hand consists of computing state variables at any integration point (element node) for a given loading history in terms of the total strain $\boldsymbol{\varepsilon}$, which is intended as a known function of the non-dimensional pseudo-time variable $t \in [0, T]$, with $t = 0$ and $t = T$ initial and final instant of the loading history, respectively. A uniform partition of the time history $[0, T]$ is considered, and for each sub-interval $[t_n, t_{n+1}]$, referred as a step, state variables at initial instant t_n, indicated by the subscript n, are assumed to be known. The advancement in time of the material state is performed updating the state variables according to the constitutive equations, given the total strain $\boldsymbol{\varepsilon}_{n+1}$ at the final instant of the current time step. Each computation is referred as an integration step. Implementation into the NICE-H8 finite element formulation, in particular, permits to update the stress $\boldsymbol{\sigma}$ and the material tangent stiffness consistent with the integration algorithm:

$$\mathbb{D} = \left.\frac{d\boldsymbol{\sigma}}{d\boldsymbol{\varepsilon}}\right|_{n+1} \tag{23}$$

required at the level of equation (12).

3.2 Double-step midpoint method

Double-step midpoint methods divide the current time interval $[t_n, t_{n+1}]$ into two intervals $[t_n, t_{n+\alpha}]$ and $[t_{n+\alpha}, t_{n+1}]$, or *sub-steps*, being $t_{n+\alpha} \in [t_n, t_{n+1}]$ the *midpoint* instant, such that:

$$\alpha = \frac{t_{n+\alpha} - t_n}{t_{n+1} - t_n}$$

In the following it will be implicitly assumed that $\alpha = 1/2$, even the formulation can be applied to a general values for $\alpha \in [0, 1]$ The integration of the evolution equations and the inherent solution is performed first for state variables values at $t_{n+\alpha}$, and subsequently at t_{n+1}. Midpoint methods have a sound mathematical structure, grant second-order accuracy and quadratic convergence. In the following we present the algorithmic procedure followed on each sub-step computation.

3.2.1 First sub-step: $[t_n, t_{n+\alpha}]$.

The rate equations (19) and (21) are integrated value with the backward Euler method over $[t_n, t_{n+\alpha}]$. This leads to the discrete rate forms:

$$\begin{cases} \mathbf{e}^p_{n+\alpha} = \mathbf{e}^p_n + \lambda_1 \mathbf{n}_{n+\alpha} \\ \boldsymbol{\alpha}_{n+\alpha} = \boldsymbol{\alpha}_n + \lambda_1 H_{kin} \mathbf{n}_{n+\alpha} \end{cases} \tag{24}$$

where λ_1 represents the plastic rate parameter increment

$$\lambda_1 = \int_{t_n}^{t_{n+\alpha}} \dot{\gamma} dt$$

Hence, the updated values for state variables at $t_{n+\alpha}$ become:

$$\begin{cases} \mathbf{s}_{n+\alpha} = 2G\left(\mathbf{e}_{n+\alpha} - \mathbf{e}^p_{n+\alpha}\right) \\ \boldsymbol{\Sigma}_{n+\alpha} = \mathbf{s}_{n+\alpha} - \boldsymbol{\alpha}_{n+\alpha} \\ \gamma_{n+\alpha} = \gamma_n + \lambda_1 \end{cases} \tag{25}$$

The computation of the plastic multiplier λ_1 is carried out resorting to a classical return map concept, i.e. the sub-step is initially supposed to be elastic, which leads to the following midpoint elastic trial state

$$\begin{cases} \mathbf{e}^{p,TR}_{n+\alpha} = \mathbf{e}^p_n \\ \mathbf{s}^{TR}_{n+\alpha} = 2G\left(\mathbf{e}_{n+\alpha} - \mathbf{e}^p_n\right) \\ \boldsymbol{\alpha}^{TR}_{n+\alpha} = \boldsymbol{\alpha}_n \\ \boldsymbol{\Sigma}^{TR}_{n+\alpha} = \mathbf{s}^{TR}_{n+\alpha} - \boldsymbol{\alpha}^{TR}_{n+\alpha} \\ \gamma^{TR}_{n+\alpha} = \gamma_n \end{cases} \tag{26}$$

If the trial solution (26) is plastically admissible, i.e.

$$\|\boldsymbol{\Sigma}^{TR}_{n+\alpha}\| \leq \sigma_{y,0} + H_{iso}\gamma^{TR}_{n+\alpha} \tag{27}$$

the state variables at $t_{n+\alpha}$ are updated with the trial ones ($\lambda_1 = 0$). If $\boldsymbol{\Sigma}^{TR}_{n+\alpha}$ violates the yield limit, a plastic correction is carried out:

$$\begin{cases} \mathbf{e}^p_{n+\alpha} = \mathbf{e}^{p,TR}_{n+\alpha} + \lambda_1 \mathbf{n}_{n+\alpha} \\ \boldsymbol{\alpha}_{n+\alpha} = \boldsymbol{\alpha}^{TR}_{n+\alpha} + H_{kin}\lambda_1 \mathbf{n}_{n+\alpha} \\ \mathbf{s}_{n+\alpha} = \mathbf{s}^{TR}_{n+\alpha} - 2G\lambda_1 \mathbf{n}_{n+\alpha} \\ \boldsymbol{\Sigma}_{n+\alpha} = \boldsymbol{\Sigma}^{TR}_{n+\alpha} - Y^{\lambda_1} \mathbf{n}_{n+\alpha} \\ \gamma_{n+\alpha} = \gamma^{TR}_{n+\alpha} + \lambda_1 \end{cases} \tag{28}$$

where the normal tensor $\mathbf{n}_{n+\alpha} = \boldsymbol{\Sigma}_{n+\alpha}/\|\boldsymbol{\Sigma}_{n+\alpha}\|$ is obtained by the co-alignment relation

$$\frac{\boldsymbol{\Sigma}_{n+\alpha}}{\|\boldsymbol{\Sigma}_{n+\alpha}\|} = \frac{\boldsymbol{\Sigma}_{n+\alpha}^{TR}}{\|\boldsymbol{\Sigma}_{n+\alpha}^{TR}\|} \tag{29}$$

while the plastic multiplier λ_1 is computed by enforcing plastic consistency $F(\boldsymbol{\Sigma}_{n+\alpha}) = 0$ for the corrected state, and, after some algebra, is given by the following expression

$$\lambda_1 = \frac{\|\boldsymbol{\Sigma}_{n+\alpha}^{TR}\| - \left(\sigma_{y,0} + H_{iso}\gamma_{n+\alpha}^{TR}\right)}{2G + H_{iso} + H_{kin}} \tag{30}$$

3.2.2 Second sub-step: $[t_{n+\alpha}, t_{n+1}]$

Solution at final instant t_{n+1} is computed with a non-standard procedure, still involving a return map projection. A non-standard endpoint *elastoplastic* trial state for history variables is computed, obeying a linear interpolation in time through values at t_n and at $t_{n+\alpha}$, namely:

$$\overline{hv}_{n+1}^{TR} = \frac{1}{\alpha}hv_{n+\alpha} - \frac{1-\alpha}{\alpha}hv_{n+1} \tag{31}$$

where the barred quantity $\overline{hv}_{n+1}^{TR}$ indicates the end-point trial value of any history variable. A return map correction is then performed directly on the trial solution (31) and enables to calculate $\bar{\lambda}_2$ which satisfies

$$\gamma_{n+1} = \bar{\gamma}_{n+1}^{TR} + \bar{\lambda}_2 \tag{32}$$

where γ_{n+1} is the plastic rate parameter at t_{n+1}, consistent with the yield surface limit. Specifically, the scheme proceeds as follows: if the barred trial relative stress $\bar{\boldsymbol{\Sigma}}_{n+1}^{TR}$ is consistent with the trial yield limit:

$$\|\bar{\boldsymbol{\Sigma}}_{n+1}^{TR}\| \leq \bar{\sigma}_{y,n+1}^{TR} = \sigma_{y,0} + H_{iso}\bar{\gamma}_{n+1}^{TR} \tag{33}$$

state variables at t_{n+1} are updated with the the trial ones. If this is not the case, a plastic correction is performed the usual form:

$$\begin{cases} \mathbf{e}_{n+1}^p = \bar{\mathbf{e}}_{n+1}^{p,TR} + \bar{\lambda}_2\mathbf{n}_{n+1} \\ \mathbf{s}_{n+1} = \bar{\mathbf{s}}_{n+1}^{TR} - 2G\bar{\lambda}_2\mathbf{n}_{n+1} \\ \boldsymbol{\alpha}_{n+1} = \bar{\boldsymbol{\alpha}}_{n+1}^{TR} + H_{kin}\bar{\lambda}_2\mathbf{n}_{n+1} \\ \boldsymbol{\Sigma}_{n+1} = \bar{\boldsymbol{\Sigma}}_{n+1}^{TR} - Y^{\bar{\lambda}_2}\mathbf{n}_{n+1} \\ \gamma_{n+1} = \bar{\gamma}_{n+1}^{TR} + \bar{\lambda}_2 \end{cases} \tag{34}$$

The endpoint unit normal to the yield domain $\mathbf{n}_{n+1}$ results

$$\mathbf{n}_{n+1} = \frac{\boldsymbol{\Sigma}_{n+1}}{\|\boldsymbol{\Sigma}_{n+1}\|} = \frac{\bar{\boldsymbol{\Sigma}}_{n+1}^{TR}}{\|\bar{\boldsymbol{\Sigma}}_{n+1}^{TR}\|}$$

while solution of the discrete plastic admissibility condition $F(\mathbf{\Sigma}_{n+1}) = 0$, gives

$$\bar{\lambda}_2 = \frac{\|\bar{\mathbf{\Sigma}}_{n+1}^{TR}\| - \left(\sigma_{y,0} + H_{iso}\bar{\gamma}_{n+1}^{TR}\right)}{2G + H_{iso} + H_{kin}} \tag{35}$$

which is substituted in (34) for state variables update at final instant. Finally the elasto-plastic material tangent stiffness $\mathbb{D}$ consistent with the algorithm is computed in closed form [8]; details are here omitted for conciseness.

4 NUMERICAL EXAMPLES

4.1 Stretched plate with circular hole

In this section we present a classic example that illustrates the capabilities of the proposed element to simulate elastoplastic media having a plate shape. Comparison are carried out using standard hexahedral eight nodes element, and the Abaqus C3D8H element. The NICE-H8 element uses 8 point of integration located at nodes and the integration rule uses weights equal to 1 [1]. A perforated strip in uniaxial tension under plane stress condition is considered. This problem is a popular benchmark used to assess accuracy and efficiency of the numerical method [9, 10, 11]. The strip has the following material properties: $E = 7000$ Kg/mm^2, $\nu = 0.2$, $\sigma_y = 24.3$ Kg/mm^2, zero hardening moduli. With reference to Figure 1(a) the following dimensions are considered: $W = 20$ mm, $L = 36$ mm, $T = 2mm$ mm and $D = 10$ mm. Due to the symmetry of the domain, only one quadrant of the strip is discretized and proper boundary conditions are considered along symmetry axes 1(b). The loading condition for the plate is an imposed displacement of 10 mm on the upper boundary of the plate AB, applied with 30 equal increments. The curves in Figure 2, reports the nodal reaction sum along side AB versus the imposed displacement, and shows a good agreement between present and reference solutions. The initial and final configuration for the plate are represented in Figure 3(a), together with equivalent plastic strain which appear to be localized at the nodes around the circular hole. It is remarked that the NICE-H8 formulation permits to recover inelastic strain and equivalent stress directly on the domain, without any post-processing, since the recovered quantities at the nodes (that is at the quadrature points) are the actual solution. The nodal values are then linearly interpolated across the faces of the elements, as it can be appreciated by inspecting Figure 3(b).
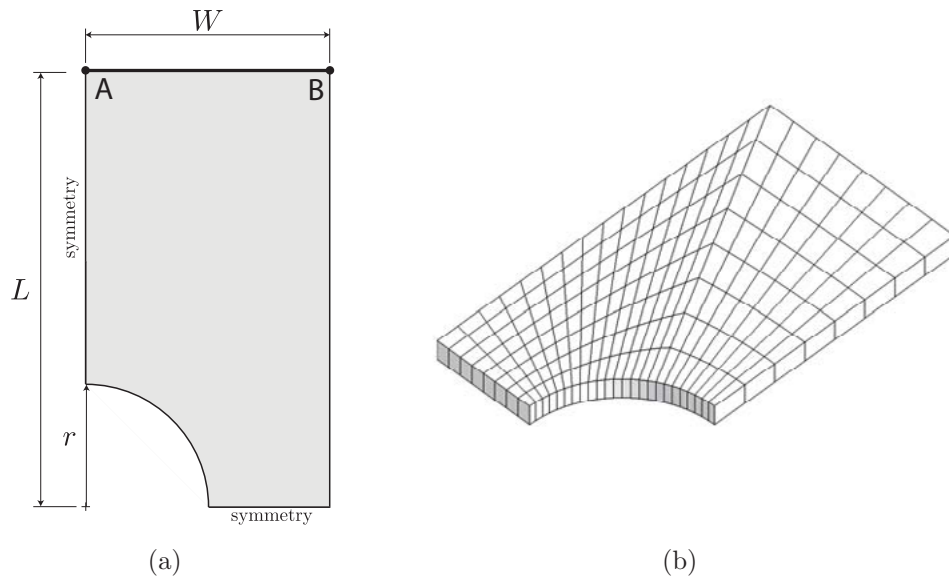
(a)   (b)

Figure 1: Stretched plate with circular hole: (a) geometry and boundary conditions (b) adopted mesh.
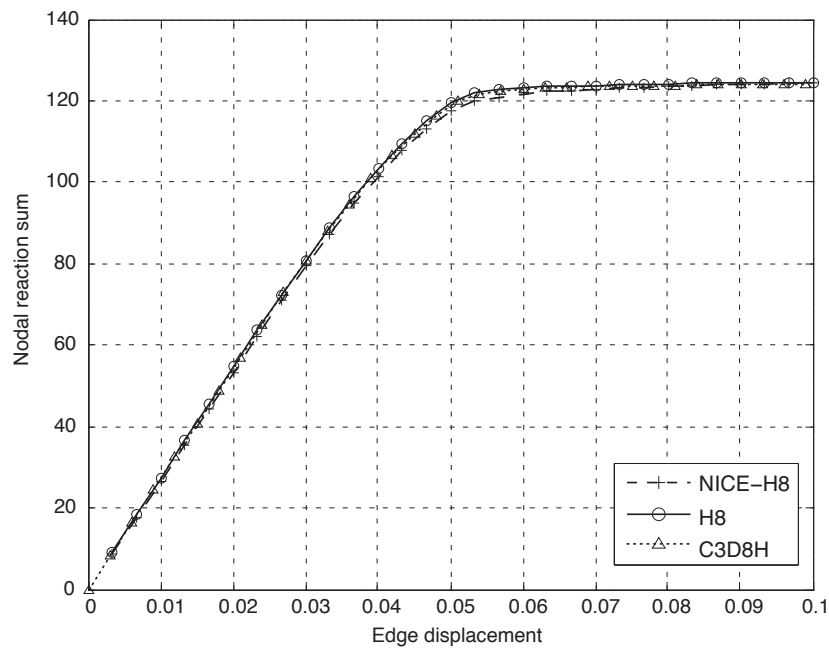

Figure 2: Stretched plate with circular hole: response curves for AB edge displacement *vs* nodal reaction sum.
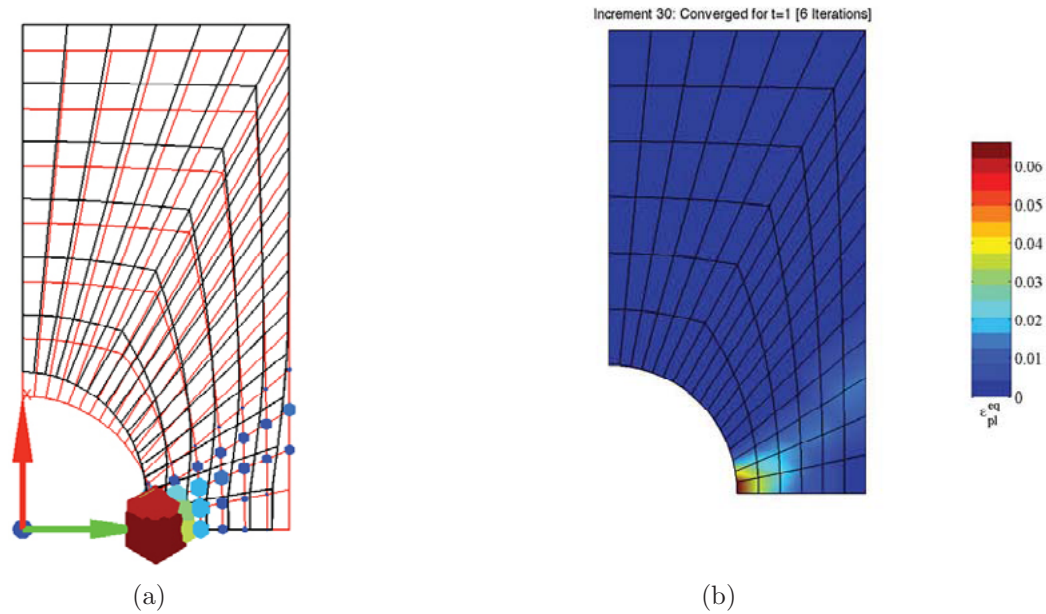
Figure 3: Stretched plate with circular hole: (a) undeformed (red) and deformed (black) configurations and equivalent plastic strain nodal localization. (b) equivalent plastic strain recovery.

5 CONCLUSIONS

In this work we have introduced the NICE-H8 linear hexahedral element based on an assumed-strain finite element technique, in conjunction with J_2 plasticity. The element approach is based on assumed gradient operators, derived via nodal integration from the kinematic-weighted residual, which leads to a pure displacement formulation. The adopted constitutive model is the classical associative von-Mises plasticity model with isotropic and kinematic hardening. A double-step midpoint integration algorithm is adopted for the integration and solution of the relevant nonlinear evolution equations. The formulation shows reliabiliy and robustness when compared to standard 3D finite element reference solution indicating its feasibility for practical application.

REFERENCES

[1] Krysl, P. and Zhu, B. Locking-free continuum displacement finite elements with nodal integration. *Int. J. Num. Meth. Engng.* (2008) **76**: 1020–1043.

[2] Broccardo, M., Micheloni M. and Krysl, P. Assumed-deformation gradient finite elements with nodal integration for nearly incompressible large deformation analysis. *Int. J. Num. Meth. Engng.* (2009) **78**: 1113–1134.

[3] Castellazzi, G. and Krysl, P. Patch-averaged assumed strain finite elements for stress analysis. *Int. J. Num. Meth. Engng.* (2012) **90**:1618–1635.

[4] Artioli, E., Auricchio F. and Beiro da Veiga L. Generalized midpoint integration algorithms for J_2 plasticity with linear hardening. *Int. J. Num. Meth. Engng.* (2007) **72**: 422–463.

[5] Lubliner, J. *Plasticity Theory*, (1990), Macmillan, New York.

[6] Simo, J.C. *Numerical analysis of classical plasticity*, Handbook for Numerical Analysis, vol. IV, 183-499, Ciarlet P.G. and Lions J.J. (eds.), (1998), Elsevier, Amsterdam.

[7] Han, W. and Daya Reddy, B. *Plasticity: mathematical theory and numerical analysis*, (1999), Springer-Verlag, New York.

[8] Artioli, E., Castellazzi, G. and Krysl, P. Assumed-strain nodally integrated hexahedral finite element formulation for elastoplastic applications. *Int. J. Num. Meth. Engng.* (2013), *submitted*.

[9] Theocaris, P.S. and Marketos, E. Elastic-plastic analysis of perforated thin strips of a strain-hardening material. *J. Mech. Phys. Sol.* (1964) **12**: 377–380.

[10] Marcal, P.V. and King, I.P., Elastic-plastic analysis of two-dimensional stress systems by the finite element method, *Int. J. Mech. Sci.* (1967) **9**: 143–155.

[11] Zienkiewicz, O. C., Valliappan, S. and King, I. P. Elasto-plastic solutions of engineering problems initial stress, finite element approach, *Int. J. Num. Meth. Engng.* (1969) **1**:75–100.